Int. j. adv. multidisc. res. stud. 2026; 6(6):743-746

Received: 28-09-2026
Accepted: 08-11-2026

International Journal of Advanced Multidisciplinary Research and Studies

ISSN: 2583-049X

Atomistic Simulation of Two-Dimensional Bi-BX (X=S, O) Nano Sheets Using the Atomic Finite Element Method

[1] Nguyen Huu Tu, [2] Nguyen Van Trang
[1] Faculty of Fundamental Science, Military Academy of Logistics, Hanoi, Vietnam
[2] Thai Nguyen University of Technology, Thai Nguyen, Vietnam

DOI: https://doi.org/10.62225/2583049X.2026.6.6.7182
Corresponding Author: **Nguyen Van Trang**

Abstract
In this study, the mechanical properties of two-dimensional Bi-BX (X=S, O) materials are investigated through atomic finite element method with Stillinger-Weber potential. The two-dimensional Young's modulus, Poisson's coefficient, maximum stress and strain of these materials are examined for two Bi-BX nanosheets. Under uniaxial tension, we have determined main mechanical properties. For Bi-BO, the maximum stress (σt) was 26.014 N/m in the armchair direction, and the maximum elastic modulus (Et) was 284.16 N/m in the zigzag direction. For Bi-BS, the maximum Poisson's ratio (ν) observed was 0.187 in the zigzag direction. The results are important information for the mechanical properties of Bi-BX nanosheets, which will be useful for their future applications.

Keywords: 2D Elastic Modulus, Poisson's Ratio, 2D Materials, AFEM, Bi-BX

1. Introduction

The discovery of two-dimensional materials with a thickness of a single atomic layer represents a breakthrough in materials science and technology. The carbon nanotubes were discovered by Iijima in the year 1991 by an early experimental observation of carbon nanotubes by TEM (Transmission electron microscopy) and the succeeding reports of conditions for the synthesis of large quantities of nanotubes [1]. This was further confirmed by the Nobel Prize in Physics awarded to the scientists Andre Geim and Konstantin Novoselov for the successful synthesis of graphene [2]. Since then, many new nanomaterials have been discovered, such as black phosphorene [3, 4], 1H [5, 6], 1T-1H [7, 8], and bi-buckled structures [9]. Among them, we are interested in Bi-BX, a two-dimensional material with a Bi-buckled structure, where B is Boron and X (S or O) belongs to Group VI. The Bi-buckled structure consists of X atoms distributed across upper and lower planes, with B atoms situated on two inner planes (sharing an axis of symmetry). Each B atom bonds to one other B atom and three surrounding X atoms, while each X atom bonds to three corresponding B atoms (Fig 1).

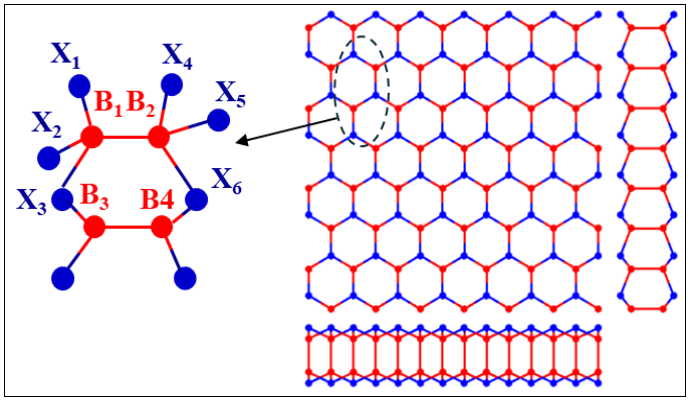

Fig 1: Structure of the Bi-Buckled materials; red represents B, and blue represents X (X = O, S)

Like other materials, 2D materials require a comprehensive characterization of their mechanical, physical, and chemical properties, as well as their stability, before being put into practical application. We focus on investigating the mechanical properties of 2D materials whose existence has been proven, as well as the feasibility of synthesizing them. At the nanometer scale, the mechanical properties of materials can be determined through ab initi calculations, experiments, and simulations. The Atomic Finite Element Method (AFEM) has been successfully employed to analyze the mechanical behavior of various hexagonal structural sheets, utilizing the Stillinger-Weber (SW) potential for 1T-ScX_2 nanostructures [10]. With the new group of Bi-buckled structured materials has received some research [9]. Jiang *et al* used molecular dynamics method with the Stillinger-Weber potential to estimate mechanical of Bi-buckled nano materials [9]. The present work investigates through atom finite element method (AFEM) the mechanical properties of Bi-buckled nanomaterials under tensile using the Stillinger-Weber potential.

2. Experimental Simulation by the Atomic Finite Element Method (AFEM)

The atomic finite element method (AFEM), combined with appropriate interatomic potential functions such as Stillinger-Weber [11], provides a reliable and efficient framework for investigating the mechanical properties of 2D materials. The basis of the atomic finite element method is to apply the principle of minimization of potential energy to the atomic interaction potential of the Bi-buckled sheet (Fig 1) to determine the stiffness matrix, then construct the overall stiffness matrix, and then apply it to the finite element equation:

$$\boldsymbol{K}^{(k)}\boldsymbol{u}^{(k)} = \boldsymbol{F}^{(k)} \quad (1)$$

With

$$\boldsymbol{K}_{ij}^{k} = \frac{\partial^2 \Pi^{(k)}}{\partial \boldsymbol{u}_i \partial \boldsymbol{u}_j}; F_i^{(k)} = -\frac{\partial \Pi^{(k)}}{\partial \boldsymbol{u}_i} = f_i - \frac{\partial E^{(k)}}{\partial \boldsymbol{u}_i} \quad (2)$$

And $\boldsymbol{K}^{(k)}$ is the overall stiffness matrix, $\boldsymbol{u}^{(k)}$ is the nodal displacement vector, and $\boldsymbol{F}^{(k)}$ is the nodal force vector.

Solving the system of equations (2), the displacement of all atoms in the sheet is determined. In the experimental simulation using the atomic finite element method, solving the system of equations (2) using the Newton-Raphson iterative method, the use of this method is clearly shown in [12, 13, 14], then the equation in finite element form is the form of equation (1).

The Stillinger-Weber (SW) potential is used to calculate the interaction potential energy between atoms. The corresponding components include: linear bonds (B-B and B-X); bond angles involving three atoms (X-B-X and B-X-B) with identical parameters (similar to the buckled material); and bond angles involving three atoms (B-B-X) - this being the distinguishing feature between the Bi-buckled and buckled structures (Fig 2).

For each Bi-buckled sheet, the atomic interaction potential is determined through the parameters of the Stillinger-Weber potential function including the direct binding energy of two adjacent atoms (E_r, eV) and the binding energy of three adjacent atoms (E_θ, eV) through the following equations:

$$E = E_r + E_\theta \quad (3)$$

$$E_r = \sum_{i=1}^{m} V_2 \quad (4)$$

$$E_\theta = \sum_{i=1}^{n} V_3 \quad (5)$$

$$V_2 = A e^{\left[\rho/(r_{ij}-r_{max})\right]}\left(B/r_{ij}^4 - 1\right) \quad (6)$$

$$V_3 = K e^{\left[\rho_{ij}/(r_{ij}-r_{max\,ij})+\rho_{ik}/(r_{ik}-r_{max\,ik})\right]}\left(\cos(\theta_{ijk}) - \cos(\theta_0)\right)^2 \quad (7)$$

In which, E is total atomic bond energy; E_θ (eV) is total angular bond energy of 3 atoms on the entire sheet; E_r(eV) is total linear bond energy between two atoms of the sheet; V_2(eV) is linear bond energy of two adjacent atoms; V_3(eV) is angular bond energy of 3 adjacent atoms; m and n are number of linear bonds and angular bonds in a calculation model; A(eV) and K(eV) are material coefficients; ρ(Å), B(Å^4), ρ_{ij}(Å), ρ_{ik}(Å), θ_o(degrees) are geometric parameters of the material; r_{ij}(Å), r_{ik}(Å) are bond length between two atoms *i, j* and *k* respectively; θ_{ijk} (degrees) is bond angle between three atoms *i, j, k* (where *i* is the middle atom).

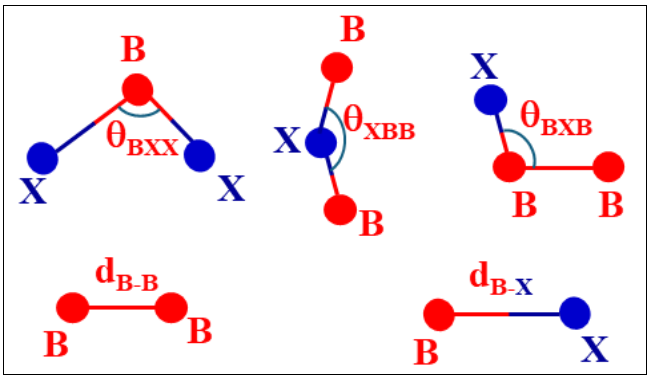

Fig 2: Elements in the calculation program represented via links

The SW potential parameter sets for Bi-BX interactions are taken from [9] and presented in Tables 1, 2, and 3. Here, the Stillinger-Weber (SW) potential is further developed to investigate the mechanical characteristics of Bi-BX nanoplates.

In the tensile experiment simulation, each Bi-BX sheet has a total number of atoms of N; the initial coordinates and displacements of the i-th atom are X_i and u_i respectively; after deformation, the coordinates of the atoms are determined as: $x_i = X_i + u_i$. The atomic interaction potential of the entire sheet calculated by formula (1) is an expression depending on the coordinates of each atom on the sheet as follows:

$$E = E(\boldsymbol{x}_1, \boldsymbol{x}_2, \ldots, \boldsymbol{x}_N) \quad (8)$$

On the other hand, when the sheet is subjected to an external force f_i on the i-th atom (considered as nodes), the atoms in the sheet have displacements of ui respectively, the potential energy of the external force is calculated as follows:

$$E_{ext} = \sum_{i=1}^{N} \boldsymbol{f}_i \boldsymbol{u}_i \quad (9)$$

On the entire sheet, the total potential energy is:

$$\Pi = E - E_{ext} \tag{10}$$

According to the principle of minimum potential energy, the sheet is in equilibrium when the total potential energy reaches its minimum value. Therefore:

$$\frac{\partial \Pi}{\partial \boldsymbol{u}_i} = 0;\ i = 1 \div N \tag{11}$$

Equation (11) is the equilibrium condition of the sheet. With the total potential energy satisfied (11), the stiffness matrix in equations (1) and (2) is completely determined.

Solve the system of equations (1) using the Newton-Raphson iterative method with boundary conditions on displacement: atoms on the tensile boundary (Fig 3) have displacement equal to u_0; atoms on the holding boundary (Fig 3) have no displacement in the tensile direction. This is the method of simulating the sheet tensile test using the atomic finite element method, thereby determining the mechanical properties of the materials under consideration.

Table 1: Bi-BX material constants (X=O, S) [9]

No	Material	a (Å)	d_{B-O} (Å)	d_{B-B} (Å)
1	Bi-BO	2.44	1.52	1.77
2	Bi-BS	3.03	1.94	1.72

Table 2: Parameters of the V_2 function for Bi-BX (X=O, S) [9]

No	Material	Bond	A (eV)	ρ (Å)	B (Å^4)	r_{min} (Å)	r_{max} (Å)
1	Bi-BO	B-O	11.725	1.207	2.669	0	2.197
		B-B	6.749	0.875	4.908	0	2.392
2	Bi-BS	B-S	13.021	1.417	7.082	0	2.769
		B-B	14.613	1.809	4.376	0	2.602

Table 3: Parameters of the V_3 function for Bi-BX (X=O, S) [9]

No	Material	Angle	K (eV)	θ (Degree)	ρ_1 (Å)	ρ_2 (Å)	r_{12min} (Å)	r_{12max} (Å)	r_{13min} (Å)	r_{13max} (Å)	r_{23min} (Å)	r_{23max} (Å)
1	Bi-BO	B-O-O	170.486	106.764	1.207	1.207	0	2.197	0	2.197	0	3.333
		B-B-O	87.662	112.059	0.875	1.207	0	2.392	0	2.197	0	3.198
2	Bi-BS	B-S-S	85.459	102.691	1.417	1.417	0	2.769	0	2.769	0	4.139
		B-B-S	102.002	115.613	1.809	1.417	0	2.602	0	2.769	0	3.717

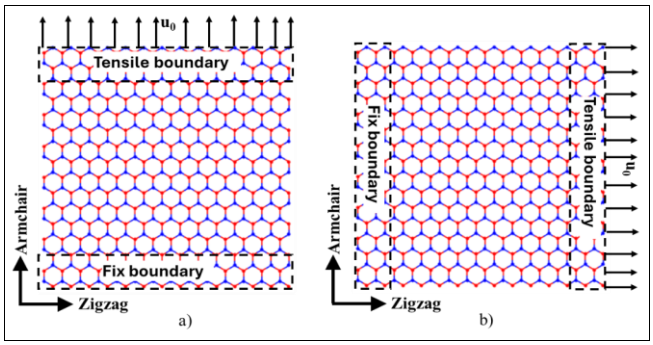

Fig 3: Sheet tensile test model Bi-BX nano materials

3. Results

Tensile tests on Bi-BX nanosheets were simulated to determine the mechanical properties of the sheets along the armchair (AC) and zigzag (ZZ) directions (Fig 3). In the simulation, pull the rectangular sheet with approximately equal side dimensions (the rectangle is considered to be a square); each sheet has 5016 atoms; each stretching step causes the atoms on the stretching edge to move with an increment of δ_ε = 0.001, repeating until the sheet has a broken bond. The atoms at the fix boundary have zero position. At each step, solve equation (12) to determine the displacement, calculate the nodal force of all atoms on the sheet at this step. The atomic displacements are then updated at every step as $x_{(k+1)} = x_{(k)} + u_{(k)}$; until $\|F^{(k)}\| \le \delta$, where δ is a given tolerance.

Upon completion of the simulation, by linearizing the stress-strain relationship within the (0-1%) range, the elastic modulus for the Bi-BO and Bi-BS sheets were determined. For the Bi-BO sheet, the elastic modulus (Et) is 282.48 when stretched along the AC direction and 284.16 when stretched along the ZZ direction. For the Bi-BS sheets, Et is 181.62 when stretched along the AC direction and 181.14 when stretched along the ZZ direction. The Poisson's ratio (ν) was calculated based on the relationship between longitudinal and transverse strains: for the Bi-BO sheet, ν=0.07 when stretched along both the AC and ZZ directions; for the Bi-BS sheet, ν=0.184 when stretched along the AC direction and ν=0.187 when stretched along the ZZ direction. The Young's modulus, fracture stress, and fracture strain of Bi-BX nanosheets in the armchair and zigzag directions are showed in Table 4. The results indicate that the fracture stress of the nanosheet in the AC direction is nearly equal to that in the ZZ direction. These findings closely align with results obtained from MD simulations for Bi-BX nanosheets [9].

Table 4: The mechanical of Bi-buckled nanomaterials by AFEM

No	Mater-ials	Dir-ect	Elastic modulus Et, N/m			Poisson's ratio			Maximum stress □t, N/m			Tensile strain		
			Our results	[9]	error (%)	Our results	[9]	error (%)	Our results	[9]	error (%)	Our results	[9]	error (%)
1	Bi-BO	AC	282.48	299.6	-5.71	0.07	0.11	-36.36	26.014	28.9	-9.986	0.1865	0.19	-1.84
		ZZ	284.16	297.7	-4.55	0.07	0.11	-36.36	25.486	28.2	-9.623	0.2105	0.24	-12.29
2	Bi-BS	AC	181.62	179.4	1.24	0.184	0.16	15	20.342	20	1.712	0.2035	0.21	-3.10
		ZZ	181.14	178.5	1.48	0.187	0.16	16.88	19.297	19.5	-1.040	0.242	0.28	-13.57

Fig 4 displays the stress-strain curves for Bi-BX sheets under armchair and zigzag tensile loading, calculated using the SW potential via the atomic finite element method (AFEM). At any given strain value, the tensile stresses along the armchair and zigzag directions are approximately equal. For all nanosheets shown in Fig 4, tensile stress increases steadily with strain up to a maximum value before dropping abruptly, indicating brittle failure. Consequently, the maximum tensile stress and the corresponding strain represent the failure stress and failure strain, respectively.

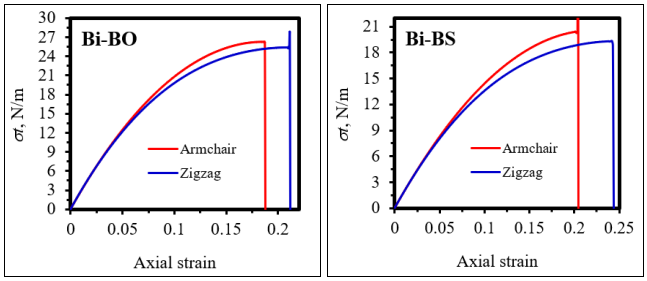

Fig 4: The stress-strain curves of Bi-buckled nanomaterials

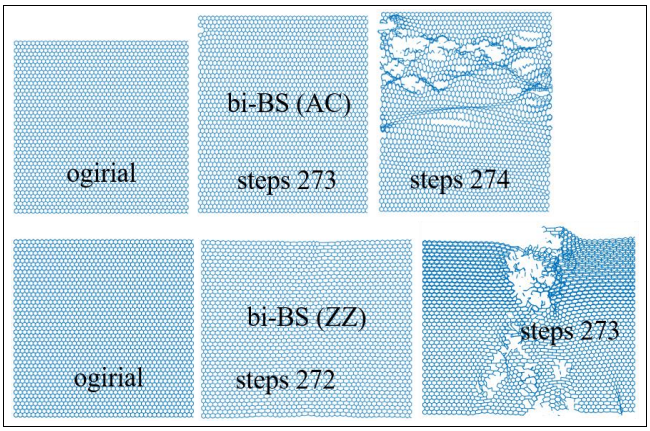

Fig 5: Broken of Bi-BS sheets

Fig 5 illustrates the failure of the bi-buckled (Bi-BS) sheet under tension. As the sheet reaches the critical strain value in both the AC and ZZ directions, cracks emerge, leading to the complete failure of the sheet. The critical strain values for both the AC and ZZ directions are approximately the same.

4. Conclusion

In this study, we employed the Atomic Finite Element Method (AFEM) with the Stillinger-Weber potential to determine the elastic modulus, fracture stress, and fracture strain of Bi-BX nanosheets along the armchair and zigzag directions. The elastic modulus along the armchair direction was found to be approximately equal to that along the zigzag direction. All sheets exhibited a brittle fracture mechanism. These mechanical properties provide crucial information for the future application of Bi-BX nanosheets.

5. Acknowledgment

This word has been supported by Thai Nguyen University of Technology and Military Academy of Logistics.

6. References

1. Iijima S. Helical microtubules of graphitic carbon. Nature. 1991; 354(6348):56-58.
2. Gokus T, *et al*. Making graphene luminescent by oxygen plasma treatment. ACS Nano. 2009; 3(12):3963-3968.
3. Lu W, *et al*. Plasma-assisted fabrication of monolayer phosphorene and its Raman characterization. Nano Research. 2014; 7(6):853-859.
4. Goren AY, *et al*. Recent progress on synthesis and properties of black phosphorus and phosphorene as new-age nanomaterials for water decontamination. ACS Applied Materials & Interfaces. 2024; 16(16):20055-20078.
5. Zamani L, *et al*. Synthesis and characterization of 5-substituted 1H-tetrazoles in the presence of nano-TiCl4. SiO_2. South African Journal of Chemistry. 2015; 68:133-137.
6. Zhan P, *et al*. Impact of synthetic CSH seeds on early hydration and pore structure evolution of cement pastes: A study by 1H low-field NMR and path analysis. Cement and Concrete Research. 2024; 175:p. 107376.
7. Wang Z, *et al*. Synthesizing 1T-1H Two-Phase Mo1-xWxS2 Monolayers by Chemical Vapor Deposition. ACS Nano. 2018; 12(2):1571-1579.
8. Thakur D, Kumar P, Balakrishnan V. Phase selective CVD growth and photoinduced 1T→ 1H phase transition in a WS 2 monolayer. Journal of Materials Chemistry C. 2020; 8(30):10438-10447.
9. Jiang J-W, Zhou Y-P. Parameterization of Stillinger-Weber potential for two-dimensional atomic crystals. arXiv preprint arXiv:1704.03147, 2017.
10. Nguyen HT. Determining the Mechanical Properties of Two-Dimensional 1T-ScX2 Materials. Engineering, Technology & Applied Science Research. 2025; 15(3):22678-22683.
11. Stillinger FH, Weber TA. Computer simulation of local order in condensed phases of silicon. Physical review B. 1985; 31(8):p. 5262.
12. Liu B, *et al*. The atomic-scale finite element method. Computer methods in applied mechanics and engineering. 2004; 193(17-20):1849-1864.
13. Wang Y, *et al*. Atomistic finite elements applicable to solid polymers. Computational Materials Science. 2006; 36(3):292-302.
14. Wackerfuß J. Molecular mechanics in the context of the finite element method. International Journal for Numerical Methods in Engineering. 2009; 77(7):969-997.